

Charging Characteristics of HTS Coil by rotary HTS Flux Pump with and without Insulation

Tue-Af-Po2.16-06 [20]

Seunghak Han¹, Haeryong Jeon¹, Ho Min Kim², Ji Hyung Kim², Yoon Seok Chae², Tae Kuk Ko¹, and Yong Soo Yoon³

1. School of Electrical and Electronic Engineering, Yonsei University, Seoul, South Korea.
3. School of Electrical Engineering, Shin Ansan University, Ansan-si, South Korea.

2. School of Electrical Engineering, Jeju National University, Jeju-si, South Korea.

September 24, 2019 from 14:00 PM to 16:00 PM



Abstract

High-temperature superconducting (HTS) coils wound without turn-to-turn insulation (NI coils) show excellent electrical and thermal performance compared to HTS coils wound with Kapton tape (INS coils). However, charging the NI coils using a direct current (DC) power supply have a slower charging time than the INS coils. To overcome this slow charging time, research is underway to charge the NI coils using a flux pump, a DC voltage source, instead of a DC power supply. In this paper, we conducted experiments to compare the charging characteristics of INS and NI coils charging by a rotary HTS flux pump. A superconducting circuit consisting of the two coils with the same magnitude of inductance is connected in series. As a result of the experiments, we compare the charging characteristics when a DC voltage source of the same value is applied to the two coils with a rotary HTS flux pump which is a contactless excitation rotary device.

I. Introduction

- No-insulation (NI) high-temperature superconducting (HTS) coils are a next-generation winding technique that can miniaturize large MRI and NMR magnets that generate conventional ultra-high-field.
- The NI magnet is driven in a driven mode that requires physical contact with the power supply (P/S), not a persistent current mode. The persistent current mode has technical difficulties because the operating current is lost to thermal energy due to joint resistance and turn-to-turn contact resistance (characteristic resistance) of the NI magnet.
- Driven mode has disadvantages such as heat load due to physical contact of the device at room and cryogenic temperatures, a complex cooling system, a need for a large power system. These drawbacks not only cause problems with the thermal and electrical stability of the system, but also increase the operating costs.
- To overcome these shortcomings, use a contactless excitation device without physical contact with the NI magnet system, which provides energy to the magnet while reducing cryogenic heat load and achieves a more important persistent current mode.
- In this study we present the charging results of two types of pancake coils. One is the NI HTS coil and the other is a pancake coil insulated using Kapton tape between turn-to-turn (INS HTS coil). In order to compare the charging results from the same power source, the charging characteristics of the rotary HTS flux pump are described by connecting the IN and INS HTS coils in series.

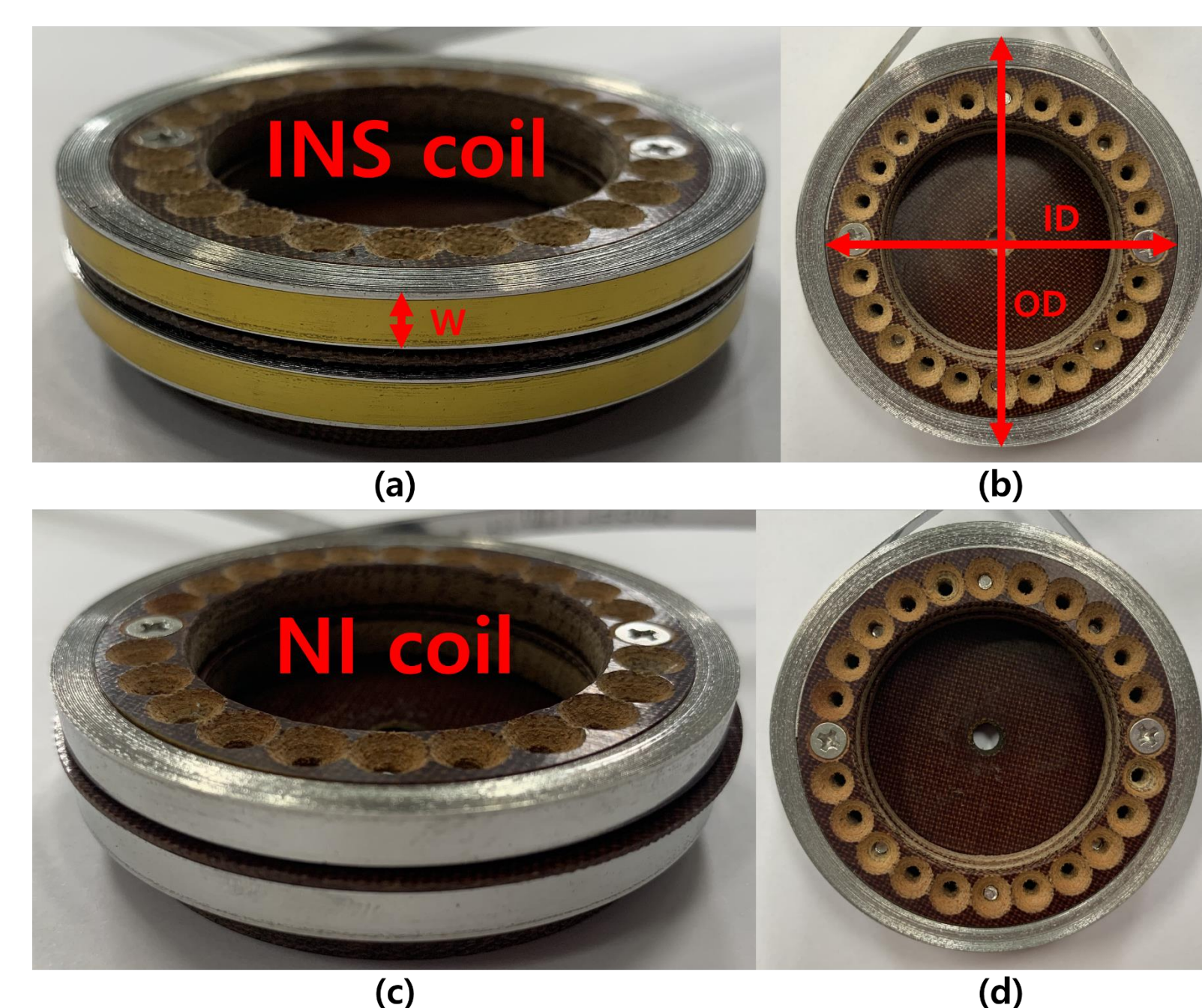


Fig. 1. Pictures of INS and NI coils.

II. Experimental setup

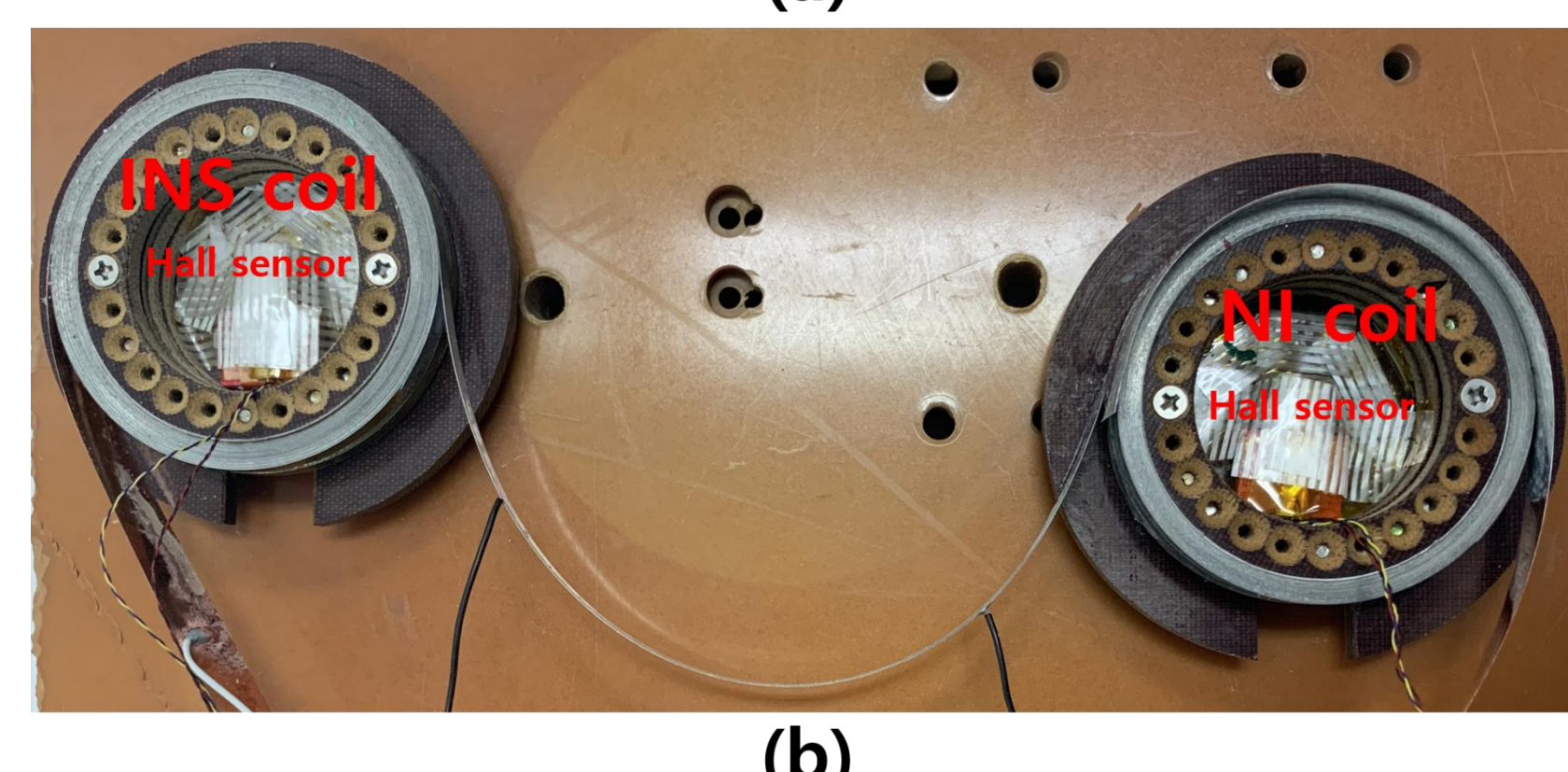
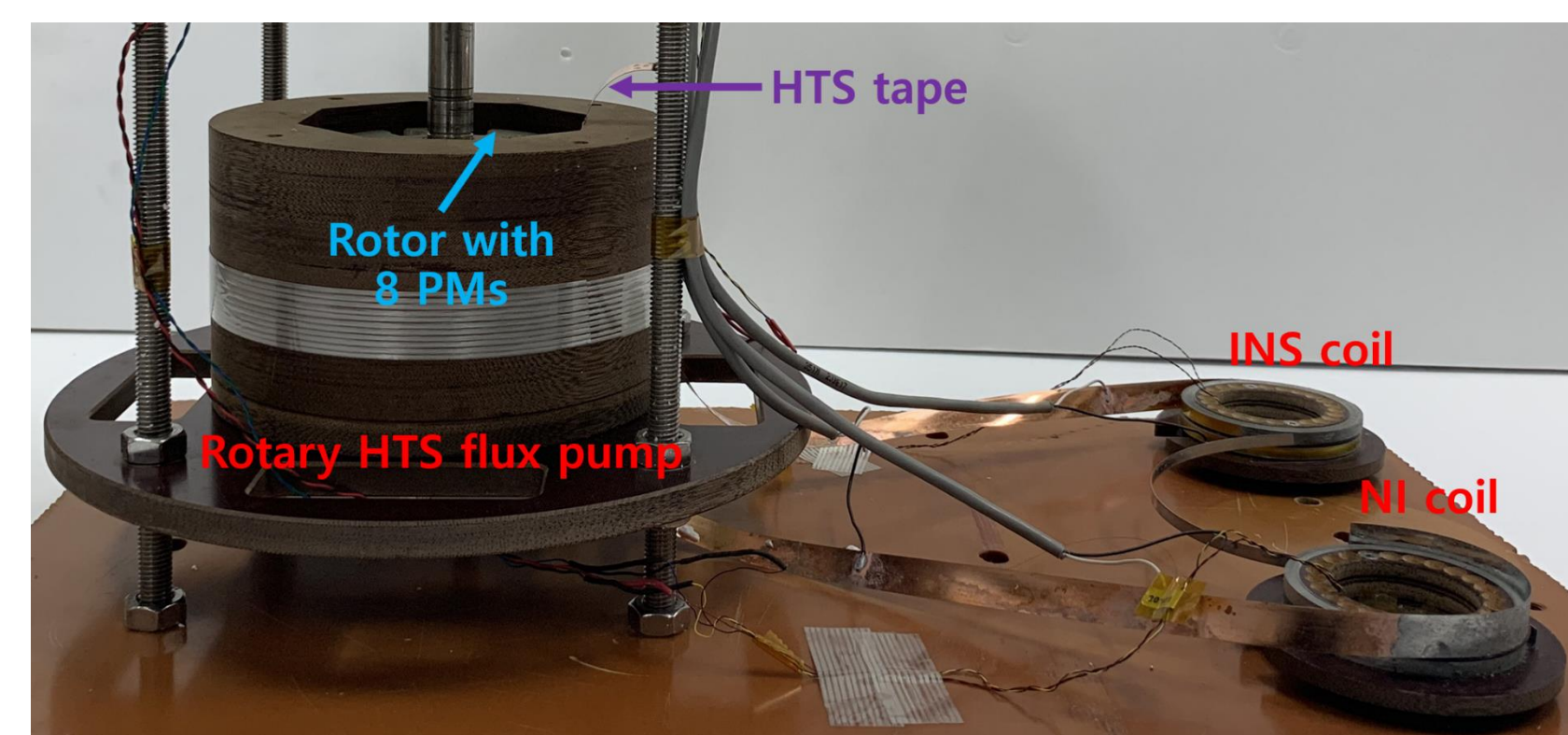


Fig. 2. Pictures of test system with INS and NI coils and a rotary HTS flux pump.

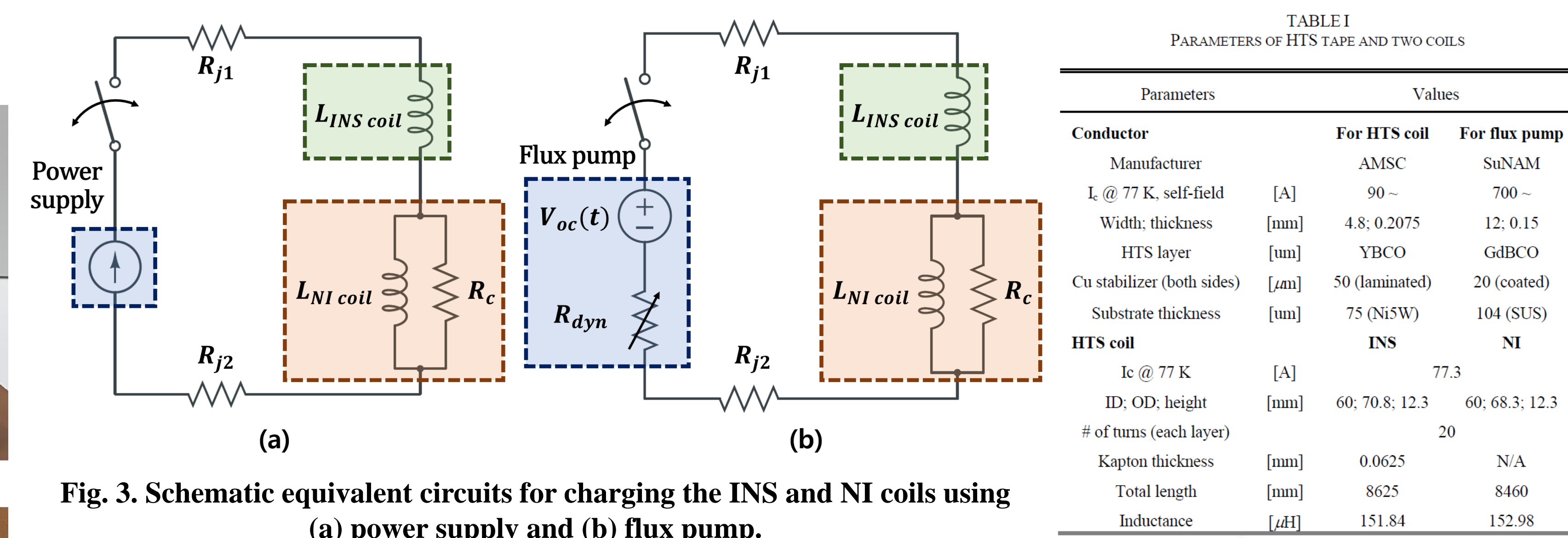


Fig. 3. Schematic equivalent circuits for charging the INS and NI coils using (a) power supply and (b) flux pump.

TABLE I PARAMETERS OF HTS TAPE AND TWO COILS		
Parameters	For HTS coil	For flux pump
Conductor	AMSC	SuNAM
I_c @ 77 K, self-field [A]	90	700
Width, thickness [mm]	4.8, 0.2075	12, 0.15
HTS layer [μm]	YBCO	GdBCO
Cu stabilizer (both sides) [μm]	50 (laminated)	20 (coated)
Substrate thickness [μm]	75 (Ni5W)	104 (SUS)
HTS coil	INS	NI
I_c @ 77 K [A]		77.3
ID, OD, height [mm]	60, 70.8, 12.3	60, 68.3, 12.3
# of turns (each layer)		20
Kapton thickness [mm]	0.0625	N/A
Total length [mm]	8625	8460
Inductance [μH]	151.84	152.98

- Fig. 2(a) shows a series connected INS and NI coils and a rotary HTS flux pump. In order to apply the same magnitude power source to both coils, it is connected in series with a rotary HTS flux pump which consists of a rotor containing eight PMs (N50) and single HTS tape.
- The air-gap, the distance between the HTS tape and the PM, is set to 5 mm, and the passing frequency of the AMF (f) is set in 10 Hz units from 10 to 100 Hz. The magnetic field of PM (N50) in 5 mm air-gap is approximately 0.21 T.
- As shown in Fig. 2 (b), the hall sensor of the lake shore is placed in the center of each coil to measure the axial magnetic field in both coils. Since the INS coil has no charging delay in the current-magnetic field, the measured magnetic field is used to calculate the magnitude of the current charged by the flux pump.
- Fig. 3(a) and (b) show the equivalent circuits for charging the INS and NI coils using a power supply and a flux pump. R_{j1} and R_{j2} are joint resistance between INS and NI coils and power source, respectively, R_{j3} is joint resistance between the coils, and R_c is turn-to-turn contact resistance of NI coil (characteristic resistance).

III. Experimental Results

A. Charging by power supply

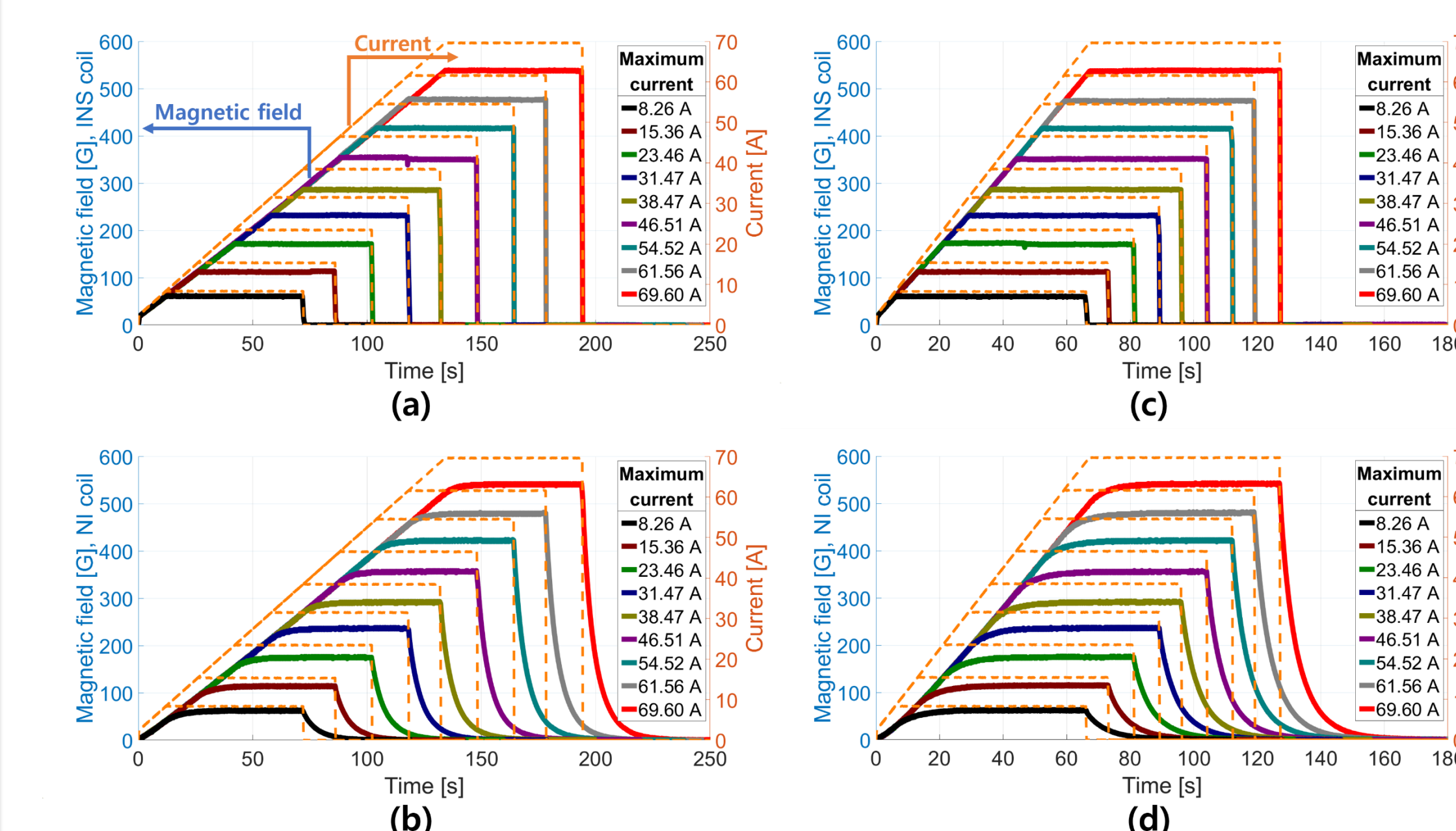


Fig. 4. Charging/discharging experimental results of (a) INS and (b) NI coils at 0.5 A/s, (c) INS and (d) NI coils at 1 A/s.

B. Charging by flux pump

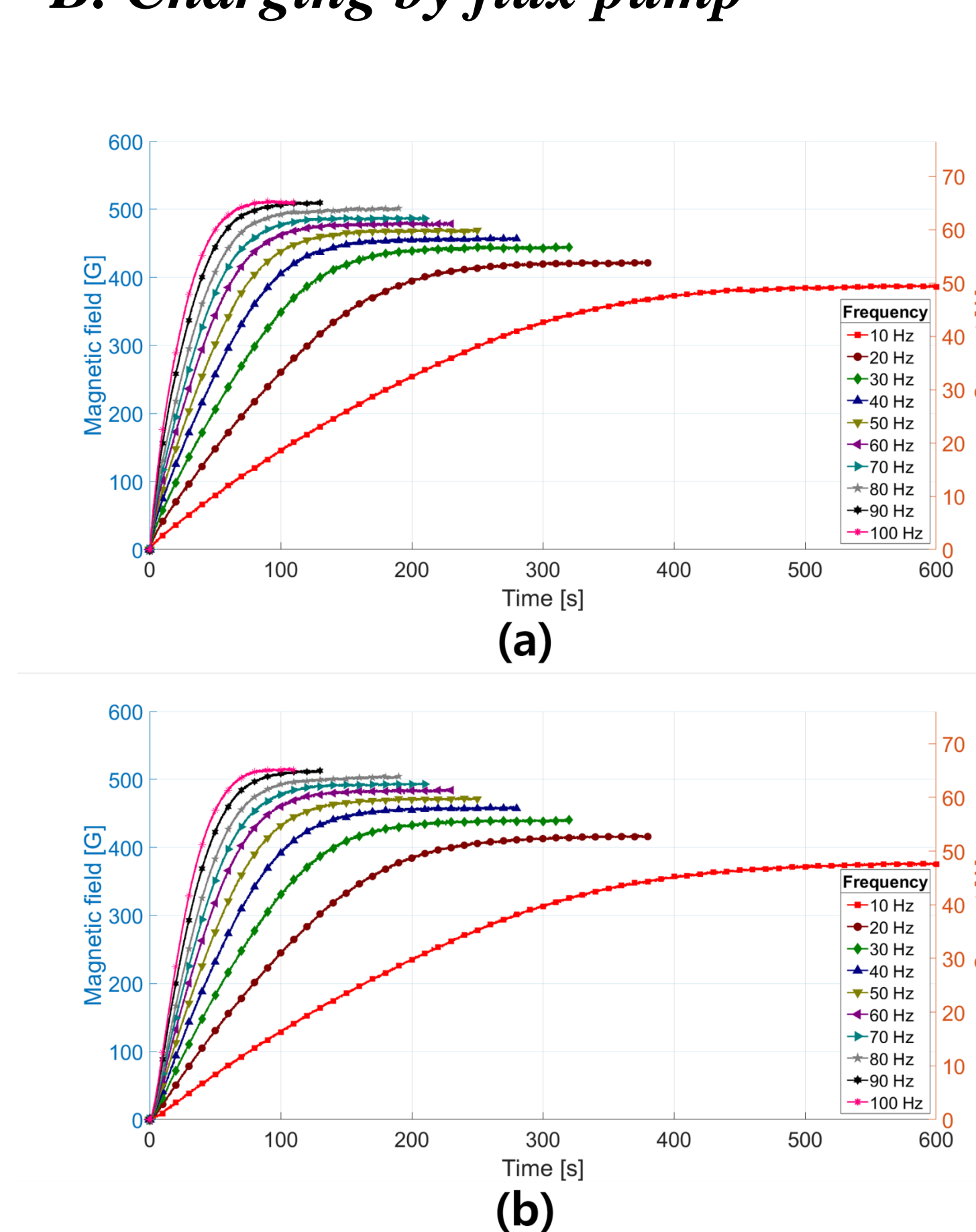


Fig. 5. Charging results of series-connected (a) INS and (b) NI coils using a rotary HTS flux pump.

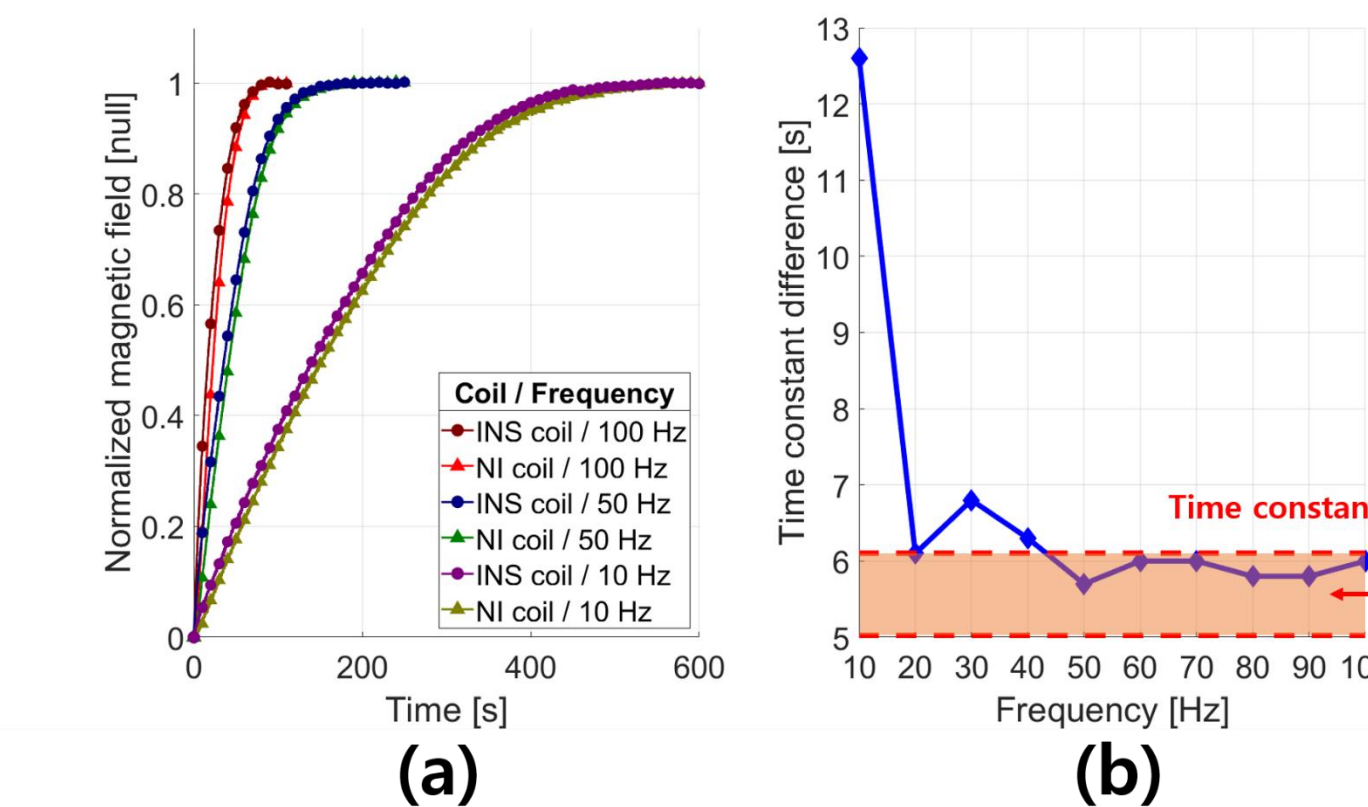


Fig. 6. (a) Time-normalized magnetic field and (b) time constant difference of the INS and NI coils according to frequency.

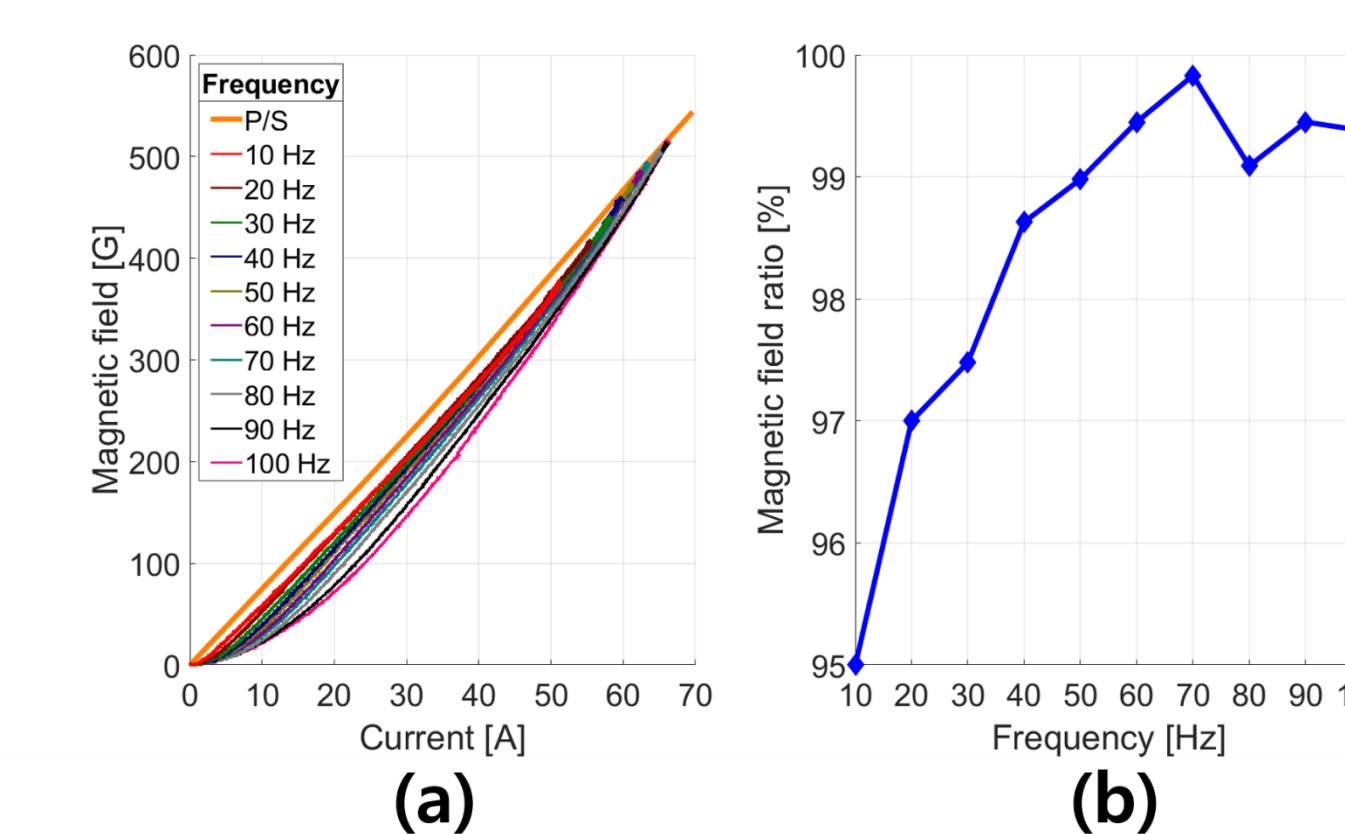


Fig. 7. Experimental results of (a) current-magnetic field and (b) magnetic field ratio using power supply and rotary HTS flux pump.

- Fig. 4 shows the charging/discharging experimental results of INS and NI coils using P/S.
- I_{op} was ramped at 0.5 and 1 A/s from 0 to maximum current (I_{max}) which was set in 10 % increments from 10 to 90 % of I_c of the HTS coil. Fig. 4(a) and (b) show the magnitudes of the current-magnetic fields of the INS and NI coils at a ramping rate of 0.5 A/s. Fig. 4(c) and (d) show the experimental results for ramping rate of 1 A/s.
- The INS coil was measured without charging/discharging delay in the current-magnetic field, but the NI coil was measured with a delay of 5.025 to 6.105 seconds time constant (τ) and summarized in Table II. τ tended to decrease as the I_{max} increased, and the experimental results showed 6.105 seconds at 8.26 A ($I_{op} / I_c : 10.69 \%$) and 5.025 seconds at 69.6 A ($I_{op} / I_c : 90.04 \%$).
- Fig. 5 shows a graph of charging results of series connected INS and NI coils using a rotary HTS flux pump. The charging experiment was carried out by setting f in 10 Hz units from 10 to 100 Hz. As shown in Fig. 5(a), the INS coil measured a saturation current (I_{sat}) of 51.4 A, a maximum magnetic field (B_F) of 387 G, and a charging time constant (τ_F) of 190.1 seconds. Fig. 5(b) shows the results of the charging experiment of the magnetic field and current of the NI coil. I_{sat} of 51.4 A, B_F of 376 G, and τ_F of 202.7 seconds was measured at 10 Hz. Even at the same current, the magnitude of BF decreased and τ_F increased.
- Fig. 6(a) shows the time-normalized magnetic field of the INS and NI coil at 10, 50, and 100 Hz. This shows the charging delay of the NI coil compared to the INS coil at each f . As shown in Fig. 6(b), the charging delay is between 5.7 and 6.8 seconds with the exception of 10 Hz, which is a similar time to charging an NI coil using P/S.
- Fig. 7(a) shows a comparison of the magnitude of the magnetic field when applying the same I_{sat} is applied to the NI coil with P/S and flux pump. As shown in Fig. 7(b), at 10 Hz, B_F by flux pump compared to B_P by P/S, B_F/B_P is 95 %, but increasing f , magnetic field ratio (B_F/B_P) increases to 99.83%.
- All numerical experimental results are summarized in Table II.

TABLE II
EXPERIMENTAL RESULTS OF INS AND NI COIL

Parameters	Values	
	INS	NI
Power source	Power supply	
HTS coil		
I_{max} [A]	8.26, 15.36, 23.46, 31.47, 38.47, 46.51, 54.52, 61.56, 69.6	
I_{max}/I_c [%]	10.69, 19.87, 30.35, 40.71, 49.77, 60.17, 70.53, 79.64, 90.04	
B_F [G]	60, 112, 170, 231, 286, 351, 415, 474, 538	62, 115, 175, 236, 291, 356, 421, 480, 544
τ_F [s]	N/A	6.105, 5.903, 5.609, 5.507, 5.451, 5.314, 5.287, 5.191, 5.025
Power source	Flux pump	
HTS coil		
f [Hz]	10, 20, 30, 40, 50, 60, 70, 80, 90, 100	
I_{sat} [A]	51.4, 55.4, 58, 59.7, 61.1, 62.3, 63.3, 65, 65.9, 66.2	
I_{sat}/I_c [%]	66.49, 71.67, 75.03, 77.23, 79.04, 80.60, 81.89, 84.09, 85.25, 85.64	
B_F [G]	387, 421, 444, 456, 469, 479, 487, 500, 509, 511	376, 416, 439, 458, 471, 483, 493, 503, 512, 514
τ_F [s]	190.1, 102.8, 73.4, 57.9, 48.9, 41.5, 36.8, 33.1, 27.9, 23.7	202.7, 108.9, 80.2, 64.2, 54.6, 47.5, 42.8, 38.9, 33.7, 29.7
$\tau_F, NI - \tau_F, INS$ [s]	12.6, 6.1, 6.8, 6.3, 5.7, 6, 6, 5.8, 5.8, 6	
B_F/B_P [%]	100	95, 97, 97.48, 98.63, 98.98, 99.45, 99.83, 99.09, 99.45, 99.38

IV. Conclusion

- The charging delay that occurs when charging the NI coil using a power supply is larger in the flux pump, but the error is small at passing frequency (f) above 20 Hz.
- At the same saturation current, the difference in maximum magnetic field occurred, but the error remained below 1 % at f above 60 Hz.
- The above drawbacks exist, but the use of flux pump reduces heat load, ensuring thermal and electrical stability of the magnet system, reducing operating costs, and achieving persistent current mode.